8-2008

Rational Design Of A Minimal Size Sensor Array For Metal Ion Detection

Manuel A. Palacios

Zhuo Wang

Victor A. Montes

Grigory V. Zyryanov

Pavel Anzenbacher Jr.
Bowling Green State University, pavel@bgsu.edu

J|A|C|S
ARTICLES

Published on Web 07/11/2008

Rational Design of a Minimal Size Sensor Array for Metal Ion Detection

Manuel A. Palacios, Zhuo Wang, Victor A. Montes, Grigory V. Zyryanov, and Pavel Anzenbacher, Jr.*

Department of Chemistry and Center for Photochemical Sciences, Bowling Green State University, Bowling Green, Ohio 43403

Received April 1, 2008; E-mail: pavel@bgsu.edu

Abstract: The focus of this study was to demonstrate that, in the luminescent sensors, the signal transduction may possibly be the most important part in the sensing process. Rational design of fluorescent sensor arrays for cations utilizing extended conjugated chromophores attached to 8-hydroxyquinoline is reported. All of the optical sensors utilized in the arrays comprise the same 8-hydroxyquinoline (8-HQ) receptor and various conjugated chromophores to yield a different response to various metal cations. This is because the conjugated chromophores attached to the receptor are partially quenched in their resting state, and upon the cation coordination by the 8-HQ, the resulting metalloquinolinolate complex displays a change in fluorescence. A delicate balance of conjugation, fluorescence enhancement, energy transfer, and a heavy metal quenching effect results in a fingerprint-like pattern of responses for each sensor-cation complex. Principal component analysis (PCA) and linear discriminant analysis (LDA) are used to demonstrate the contribution of individual sensors within the array, information that may be used to design sensor arrays with the smallest number of sensor elements. This approach allows discriminating between 10 cations by as few as two or even one sensor element. Examples of arrays comprising various numbers of sensor elements and their utility in qualitative identification of Ca^{2+}, Mg^{2+}, Cd^{2+}, Hg^{2+}, Co^{2+}, Zn^{2+}, Cu^{2+}, Ni^{2+}, Al^{3+}, and Ga^{3+} ions are presented. A two-member array was found to identify 11 analytes with 100% accuracy. Also the best two of the sensors were tested alone and both were found to be able to discriminate among the samples with 99% and 96% accuracy, respectively. To illustrate the utility of this approach to a real-world application, identification of enhanced soft drinks based on their Ca^{2+}, Mg^{2+}, and Zn^{2+} cation content was performed. The same approach to reducing array elements was used to construct three- and two-member arrays capable of identifying these complex analytes with 100% accuracy.

Introduction

The heightened concern for human health and the environmental pollution has stimulated active research on the potential impact of heavy metals and their toxic effects. Heavy metal pollution can arise from many sources, both anthropogenic as well as natural.[1] Among the most common sources are mining and purification of metals, acid mine drainages, industrial waste streams, and other sources.[2,3] Heavy metal poisoning[4] corresponds usually with accumulation of heavy metals in the soft tissues of the body and could cause serious damage to the developing brain.[5,6] Fish consumption advisories exist in many countries warning children and pregnant women to avoid eating certain fish species.[7]

Although aluminum is not a heavy metal, it makes up about 8% of the surface of the Earth and is the third most abundant element. Studies began to emerge about 20 years ago suggesting that aluminum might have a possible connection with developing Alzheimer's disease when significant amounts of aluminum were found in brain tissue of Alzheimer's patients.[8]

Due to the potential impact of metal ions on human health and environment, sensitive methods of their detections are widely sought.[9] Here, the optical detection,[10] particularly

(1) (a) *Heavy Metals in the Environment: Origin, Interaction and Remediation*; Bradl, H.; Ed.; Interface Science and Technology, Volume *6*; Elsevier: Amsterdam, 2005. (b) Wright, D. A.; Welbourn, P. *Environmental Toxicology*; Cambridge University Press: Cambridge, 2002.

(2) (a) Pacyna, E. G.; Pacyna, J. M.; Fudala, J.; Strzelecka-Jastrzab, E.; Hlawiczka, S.; Panasiuk, D.; Nitter, S.; Pregger, T.; Pfeiffer, H.; Friedrich, R. *Atmos. Environ.* **2007**, *41*, 8557–8566. (b) *Ullmann's Encyclopedia of Industrial Chemistry*, 6th ed.; Wiley VCH: New York, 1999.

(3) Marchand, E. A.; Dinkelman, I. *Water Environ. Res.* **2006**, *78*, 1654–1698.

(4) (a) *Handbook on the Toxicology of Metals*, 3rd ed.; Fowler, B. A., Nordberg, M., Friberg, L., Nordberg, G., Eds.; Academic Press: Burlington, MA, 2007. (b) Jaerup, L. *Brit. Med. Bul.* **2003**, *68*, 167–182.

(5) Rasmussen, R. S.; Nettleton, J.; Morrissey, M. T. *J. Aquat. Food Prod. Technol.* **2005**, *14*, 71–100.

(6) Vahter, M.; Berglund, M.; Akesson, A.; Liden, C. *Environ. Res.* **2002**, *88*, 145–155.

(7) (a) US EPA Document EPA-823-R-04−005, March 2004. (b) US FDA Center for Food Safety and Applied Nutrition: http://www.cfsan.fda.gov/seafood1.html.

(8) (a) Shcherbatykh, I.; Carpenter, D. O. *J. Alzheimer's Dis.* **2007**, *11*, 191–205. (b) Miu, A. C.; Benga, O.; Miu, A. C.; Benga, O. *J. Alzheimer's Dis.* **2006**, *10*, 179–201.

(9) Barile, F. A. *Principles of Toxicology Testing*; CRC Press: Boca Raton, FL, 2008.

(10) (a) Borisov, S. M.; Wolfbeis, O. S. *Chem. Rev.* **2008**, *108*, 423–461. (b) Oehme, I.; Wolfbeis, O. S. *Mikrochim. Acta* **1997**, *126*, 177–192.

fluorescence methods, shows unique potential for high sensitivity.[11] The power of optical sensors was recently augmented by implementation of sensor array technologies[12] and pattern recognition methods[13] that allow for identification of multiple metal ions using a single device.[14,15] Development of a successful optical sensor array requires sensor elements capable of sufficient discrimination of the target analytes. Sensor elements with high discriminatory capability would allow for lowering the number of sensor elements required.

In the past, we have demonstrated that a rational design of the signal transduction scheme may result in an improved sensor performance.[16] In this study, we try to make a case for the sensor design aimed at improved signal transduction scheme[16a,17] rather than increasing the receptor-substrate affinity and selectivity, as the improved selectivity via receptor modification usually results in high cost of synthesis[18] and a potential loss of a real-time response due to slow dissociation of the substrate-receptor complex,[19] which in an extreme case may render the sensor an irreversible indicator. We build on our previous experience with quinolinolate materials[16a,20] to demonstrate the advantage of the signal transduction design to generate sensors suitable for arrays comprising a minimal number of sensor elements. We will use principal component analysis (PCA)[21] and/or linear discriminant analysis (LDA)[21] to demonstrate how the sensors and their emissive properties impact the discrimination properties of the resulting arrays. Obviously, the lower the number of the sensor elements in the array, the easier the data analysis. Therefore, one of the goals of this study is to design an array with the lowest possible number of sensors capable of identification of 10 various metals.

Experimental Section

Sensors **S2**−**S6** were synthesized following the procedures described previously.[16a] **S1** is commercially available from Aldrich Chemicals. The array chips were fabricated by ultrasonic drilling of microscope slides (well diameter: 500 ± 10 μm, depth: 500 ± 10 μm). The wells were filled with 200 nL (approximately 0.08% sensor in polyurethane, w/w) in a Tecophilic THF solution (4% w/w) and dried to form a 5 μm thick polymer film in each well. In a typical assay, the cations were added as aqueous solutions (200 nL, 1 mM, pH 5) of their chloride salts to each well containing a sensor. Images from the sensor arrays were recorded using a Kodak Image Station 440CF. The sensor arrays were excited with a broadband UV lamp (300−400 nm, λ_{max} = 365 nm) and an emission intensity in three channels was utilized for signal output using the following filters: (**B**) Blue: band-pass filter 380−500 nm λ_{max} = 435 nm, (**G**) Green: band-pass filter 480−600 nm λ_{max} = 525 nm, (**Y**) Yellow: low pass filter 523 nm. After acquiring the images, the integrated (nonzero) gray pixel (n) value[22] was calculated for each well of each channel. Images of the sensor chip were recorded before (b) and after (a) the addition of analyte and their relative intensities (R) were calculated as follows:

$$R = \sum_n \frac{a_n}{b_n} - 1 \qquad (1)$$

Fluorescence excitation−emission maps were recorded by a single photon counting spectrofluorometer from Edinburgh Analytical Instruments (FL/FS 920). The range of excitation wavelength is from 230 to 415 nm in 5 nm steps, and the range of emission wavelength is from 420 to 700 nm in 1 nm steps. A 395 nm filter was used. THF was used as a solvent in all fluorimetric experiments and the counterion varies due to solubility issues of the metal ion salts in THF. For more details see the Supporting Information.

Results and Discussion

The present sensors utilize a common receptor, 8-HQ, substituted in the 5-position with an extended conjugated fluorophore such as pyrene or a fluorene fragment that emits blue fluorescence. 8-HQ does not yield appreciable fluorescence above 300 nm.[23] In general, the corresponding quinolinolate anion displays luminescence modulated by the metal ion. Hence, upon metal ion coordination by 8-HQ, a second chromophore, metalloquinolinolate, is formed. From the sensor array perspective, 8-HQ has a high potential for use in the design of

(11) (a) Wang, B.; Wasielewski, M. R. *J. Am. Chem. Soc.* **1997**, *119*, 12–21. (b) Chen, L. X.; Jäger, W. J.; Niemczyk, H. M. P.; Wasielewski, M. R. *J. Phys. Chem. A* **1999**, *103*, 4341–4351. (c) Chen, L. X.; Jäger, W. J.; Gosztola, D. J.; Niemczyk, H. M. P.; Wasielewski, M. R. *J. Phys. Chem. B* **2000**, *104*, 1950–1960. (d) Ewbank, P. C.; Loewe, R. S.; Zhai, L.; Reddinger, J.; Sauve, G.; McCullough, R. D. *Tetrahedron* **2004**, *60*, 11269–11275.
(12) Schena, M. *Microarray Analysis*; Willey-Liss: Hoboken, NJ, 2003.
(13) (a) Lavigne, J. J.; Anslyn, E. V. *Angew. Chem., Int. Ed.* **2001**, *40*, 3118. (b) Wright, A. T.; Anslyn, E. V *Chem. Soc. Rev.* **2006**, *35*, 14–28.
(14) (a) Garcia-Acosta, B.; Martinez-Manez, R.; Sancenon, F.; Soto, J.; Rurack, K.; Spieles, M.; Garcia-Breijo, E.; Gil, L. *Inorg. Chem.* **2007**, *46*, 3123–3135. (b) Carofiglio, T.; Fregonese, C.; Mohr, G. J.; Rastrelli, F.; Tonellato, U. *Tetrahedron* **2006**, *62*, 1502–1507. (c) Lee, J. W.; Lee, J.-S.; Kang, M.; Su, A. I.; Chang, Y.-T. *Chem.−Eur. J.* **2006**, *12*, 5691–5696. (d) Mayr, T.; Igel, C.; Liebsch, G.; Klimant, I.; Wolfbeis, O. S. *Anal. Chem.* **2003**, *75*, 4389–4396. (e) Mayr, T.; Liebsch, G.; Klimant, I.; Wolfbeis, O. S. *Analyst* **2002**, *127*, 201–203. (f) Szurdoki, F.; Ren, D.; Walt, D. R. *Anal. Chem.* **2000**, *72*, 5250–5257.
(15) (a) Christodoulides, N.; Tran, M.; Floriano, P. N.; Rodriguez, M.; Goodey, A.; Ali, M.; Neikirk, D.; McDevitt, J. T. *Anal. Chem.* **2002**, *74*, 3030–3036. (b) Goodey, A. P.; McDevitt, J. T. *J. Am. Chem. Soc.* **2003**, *125*, 2870–2871. (c) Chapman, P. J.; Long, Z.; Datskos, P. G.; Archibald, R.; Sepaniak, M. J. *Anal. Chem.* **2007**, *79*, 7062–7068. (d) Basabe-Desmonts, L.; Baan, F.; Zimmerman, R. S.; Reinhoudt, D. N.; Crego-Calama, M. *Sensors* **2007**, *7*, 1731–1746.
(16) (a) Palacios, M. A.; Wang, Z.; Montes, V. A.; Zyryanov, G. V.; Hausch, B. J.; Jursikova, K.; Anzenbacher, P., Jr *Chem. Commun* **2007**, 3708–3710. (b) Palacios, M. A.; Nishiyabu, R.; Marquez, M.; Anzenbacher, P., Jr *J. Am. Chem. Soc.* **2007**, *129*, 7538–7544. (c) Zyryanov, G. V.; Palacios, M.; Anzenbacher, P., Jr *Angew. Chem., Int. Ed.* **2007**, *119*, 7995–7998.
(17) (a) Pohl, R.; Aldakov, D.; Kubát, P.; Jursíková, K.; Marquez, M.; Anzenbacher, P., Jr *Chem. Commun.* **2004**, 1282–1283. (b) Aldakov, D.; Anzenbacher, P., Jr *J. Am. Chem. Soc.* **2004**, *126*, 4752–4753.
(18) (a) Bronson, R. T.; Bradshaw, J. S.; Savage, P. B.; Fuangswasdi, S.; Lee, S. C.; Krakowiak, K. E.; Izatt, R. M. *J. Org. Chem.* **2001**, *66*, 4752–4758. (b) Prodi, L.; Montalti, M.; Zaccheroni, N.; Bradshaw, J. S.; Izatt, R. M.; Savage, P. B. *Tetrahedron Lett.* **2001**, *42*, 2941–2944. (c) Bordunov, A. V.; Bradshaw, J. S.; Zhang, X. X.; Dalley, N. K.; Kou, X.; Izatt, R. M. *Inorg. Chem.* **1996**, *35*, 7229–7240. (d) Su, N.; Bradshaw, J. S.; Zhang, X. X.; Song, H.; Savage, P. B.; Xue, G.; Krakowiak, K. E.; Izatt, R. M. *J. Org. Chem.* **1999**, *64*, 8855–8861. (e) Blake, A. J.; Bencini, A.; Caltagirone, C.; De Filippo, G.; Dolci, L. S.; Garau, A.; Isaia, F.; Lippolis, V.; Mariani, P.; Prodi, L.; Montalti, M.; Zaccheroni, N.; Wilson, C. *Dalton Trans.* **2004**, *17*, 2771–2779.
(19) Swager, T. M. *Acc. Chem. Res.* **1998**, *31*, 201–207.
(20) (a) Montes, V. A.; Pohl, R.; Shinar, J.; Anzenbacher, P., Jr *Chem.−Eur. J.* **2006**, *12*, 4523–4535. (b) Pohl, R.; Montes, V. A.; Shinar, J.; Anzenbacher, P., Jr *J. Org. Chem.* **2004**, *69*, 1723–1725. (c) Pohl, R.; Anzenbacher, P., Jr *Org. Lett.* **2003**, *5*, 2769–2772.
(21) (a) Beebe, K. R.; Pell, R. J.; Seasholtz, M. B. In *Chemometrics: a practical guide*; Wiley: New York, 1998. (b) Otto, M. In *Chemometrics: Statistics and computer application in analytical chemistry*; Wiley-VCH: New York, 1999. (c) Jambu, M. In *Exploratory and Multivariate Data Analysis*; Academic Press: San Diego, 1991.
(22) The gray pixel value is a numerical value of the grey shade that for a 12-bit pixel depth detector ranges between 0 and 4095.
(23) (a) Bardez, E.; Devol, I.; Larrey, B.; Valeur, B. *J. Phys. Chem. B* **1997**, *101*, 7786–7793. (b) Valeur, B.; Badaoui, F.; Bardez, E.; Bourson, J.; Boutin, P.; Chatelain, A.; Devol, I.; Larrey, B.; Lefèvre, J. P.; Soulet, A. In: Desvergne, J.-P., Czarnik, A. W., Eds. *Chemosensors of Ion and Molecule Recognition*; NATO ASI Series; Kluwer: Dordrecht, 1997; p 195.

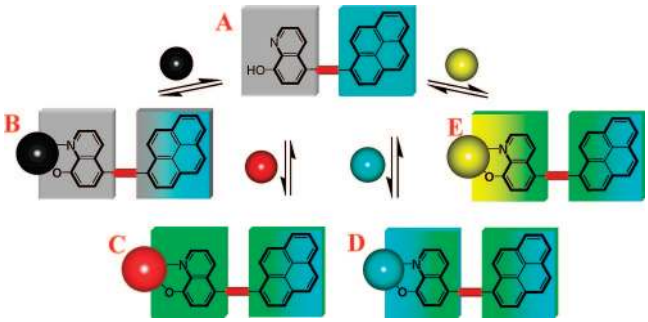

Figure 1. Upon the cation coordination by the 8-hydroxyquinoline the metalloquinolinolate complex displays a change in fluorescence. The balance between the original fluorescence of the conjugated chromophore (A) and the newly established metalloquinolinolate complexes (B−E) provide for a unique ratiometric response.

fluorescence-based sensor arrays as it shows a *turn-on* signal and is highly cross-reactive, that is, binds a number of metals while emitting light of slightly different luminescence quantum yield and wavelength for each metal. The relative contribution of the two chromophores (e.g., pyrene and metalloquinolinolate, Figure 1) to the fluorescent output depends on the nature of the metal ion including its electropositivity,[24] spin−orbit coupling,[25] and the excitation wavelength. Metal electropositivity defines whether the quinolinolate emission will be more blue-emitting as it is in the case of Mg^{2+}, green as in the case of Al^{3+}, or rather yellow-emitting as in the case of Zn^{2+}.[24] Spin−orbit coupling then defines whether the metalloquinolinolate complex will display fluorescence (e.g., Mg^{2+}, Ca^{2+}, Al^{3+}, Ga^{3+}) or rather red-shifted phosphorescence (Ir^{3+}, Pt^{3+}). However, not all phosphorescence quantum yields are high enough for the phosphorescence to be observed. Metals such as Hg^{2+} or Ni^{2+} usually quench the sensor luminescence, albeit with different efficiency.[14a,25]

Finally, the excitation wavelength determines, which part of the sensor is preferentially excited and, in the absence of energy transfer, emits light. A higher extinction coefficient (ϵ) of the organic fluorophore in the UV-region (250−370 nm) results in prevalent blue emission from the aromatic part while the excitation of the metalloquinolinolate $\pi-\pi^*$ transitions in the Near-UV and Vis-region (350−410 nm) results in a turquoise-green emission of the quinolinolate complex. Since both the receptor and aromatic fluorophore are partly conjugated, excited-state mixing and the corresponding emission may also be observed. One can also use a broadband excitation source such as a UV-lamp or multiple LEDs to excite both types of absorption in the sensors.

From the above considerations one can easily glean that the sensors utilizing an 8-HQ receptor with an attached fluorescent moiety can yield a plethora of changes and perturbations in the luminescence signal output. We show how the discriminative power of the array utilizing the above fluorescent sensors is increased by taking advantage of the cross-reactivity of the signaling.

Because metalloquinolinolates are weakly emitting ($\Phi < 0.15$),[25,26] it is desirable to attach a conjugated chromophore to boost their luminescence output. Sensors **S2**−**S6**[14a] with an extended conjugated chromophore show only weak fluorescence in solution ($\Phi_{S4} \approx 0.02$, $\Phi_{S5} \approx 0.05$) as the 8-HQ moieties exert some degree of intramolecular quenching to pyrene (**S2**) and the fluorene bridges in **S4**−**S6**. However, with an extended fluorene bridge, this quenching is not complete (Figure 2, 3).

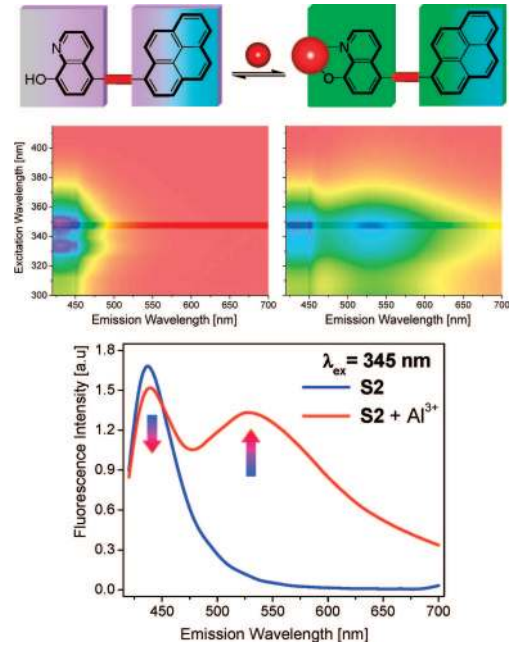

Figure 2. Upon the $AlCl_3$ cation coordination by 8-hydroxyquinoline, the Al^{3+}-quinolinolate complex of **S2** (0.5 μM) displays a change in fluorescence. The balance between the original fluorescence of the conjugated chromophore and the newly established metalloquinolinolate complexes provides for a unique ratiometric response.

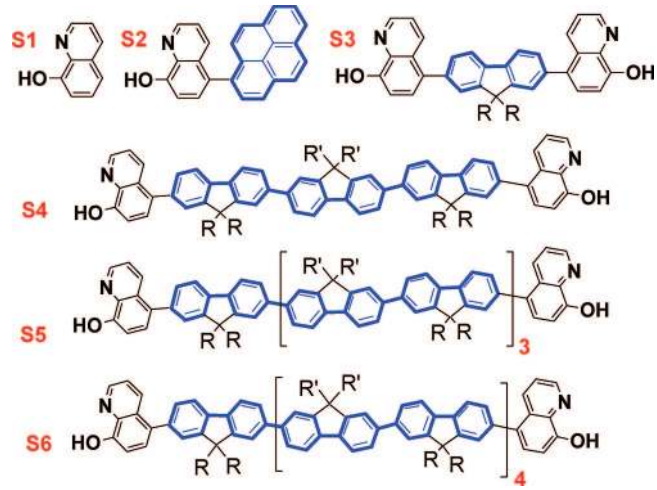

Figure 3. Structures of sensor **S1** (8-hydroxyquinoline, 8-HQ), and 8-HQ-based sensors **S2**−**S5**. R = rac-2-ethylhexyl, R′= *n*-hexyl. The extended conjugated chromophore is shown in blue color.

8-HQ is known to form luminescent chelates with a number of metal ions including Cd^{2+}, Zn^{2+}, Mg^{2+}, Al^{3+}, Ga^{3+}, In^{3+}, Sn^{4+}, Ti^{4+}, etc.[27] To prove our signal transduction concept, we selected 10 metal ions known to form luminescent complexes such as Ca^{2+}, Cd^{2+}, Mg^{2+}, Al^{3+}, and Ga^{3+}, and to a lesser extent, also Zn^{2+}, and also metal ions such as Hg^{2+}, Cu^{2+}, Ni^{2+}, and Co^{2+} that are known to quench the emission of the

(24) Chen, C. H.; Shi, J. *Coord. Chem. Rev.* **1998**, *171*, 161–174.
(25) Ballardini, R.; Varani, G.; Indelli, M. T.; Scandola, F. *Inorg. Chem.* **1986**, *25*, 3858–3865.
(26) Onoue, Y.; Hiraki, K.; Morishige, K.; Nishikawa, Y. *Nippon Kagaku Kaishi* **1978**, 1237–1241.
(27) Soroka, K.; Vithanage, R. S.; Phillips, D. A.; Walker, B.; Dasgupta, P. K. *Anal. Chem.* **1987**, *59*, 629–636.

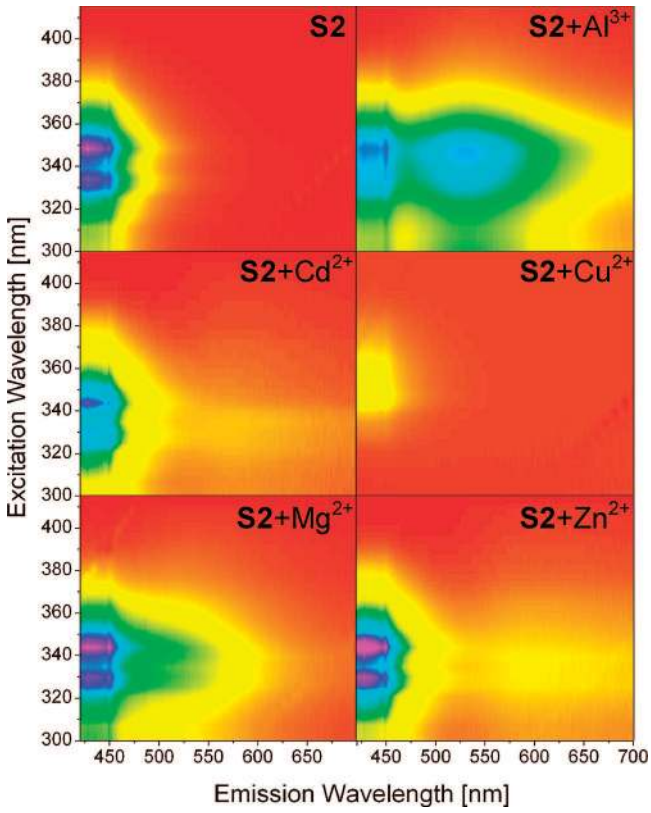

Figure 4. Fluorescence excitation−emission map for **S2**, **S2**+Al^{3+}, **S2**+Cd^{2+}, **S2**+Cu^{2+}, **S2**+Mg^{2+}, and **S2**+Zn^{2+} (**S2** (0.5 uM) with M^{2+} (50 equiv)) in dry THF. The range of the excitation wavelength is from 300 to 415 nm in 5 nm steps, and the range of emission wavelength is from 420 to 700 nm in 1 nm steps.

quinolinolate anion. The main question to be answered in this study was how many sensors were needed to achieve discrimination among the 10 cations of the above group. The success criterion is the 100% classification of the trials by the array.

Cross-reactive signal output was confirmed in solution prior to array fabrication. The method of excitation−emission maps was used to compare the emission from the sensors and the corresponding complexes. Figure 4 shows the excitation−emission maps corresponding to the changing ratios of the blue (turquoise) component of the extended chromophore, and the green (yellow) component of the metalloquinolinolate. Figure 4 illustrates how this ratiometric output, together with metal-specific attenuation or growth in the luminescence intensity, results in a high information density output signal that can be harnessed to provide the desired discrimination power of such sensors.

Although the data from the excitation−emission maps could also be used for metal identification, the goal of our efforts is a microarray device fabricated using the sensors **S1**−**S6**. The solid-state array was fabricated as reported previously using sensors **S1**−**S6** dispersed in a hydrophilic polyurethane carrier (0.07% **S2**−**S6** in polyurethane, w/w).[28,14] The purpose of the hydrophilic polyurethane is to draw in water together with the metal ions while aiding in the formation of the metalloquinolinolate complexes, and to overcome the incompatibility in solubility of the lipophilic sensors and hydrophilic cations. The luminescence from the array was recorded upon exposure to 10 metal cations: Ca^{2+}, Mg^{2+}, Cd^{2+}, Hg^{2+}, Co^{2+}, Zn^{2+}, Cu^{2+}, Ni^{2+}, Al^{3+}, and Ga^{3+}, as their chloride salts in water (1 mM in water, 200 nL, 7 trials each). We have tested pH=5, 6, and 7 of the analyte solution and decided to work with pH = 5, as at pH = 6 and 7 some metal ions started to precipitate as hydroxides. Figure 5 shows responses of **S1**−**S6** in blue, green, and yellow channels to the cation solutions, and the corresponding changes in a yellow channel at pH = 5 as an example of the raw data.

As predicted, each of the metal cations induced a different pattern of luminescence changes in the individual sensors of the array, thus creating a multidimensional response pattern (Figure 5, left). As an example, Figure 5 also shows the response pattern generated by the sensor array in the presence of Mg^{2+}. Supporting Information shows the response patterns generated by all of the metal cations in all of the sensors. Inspection of the patterns reveals that **S2** is the most sensitive sensor for Mg^{2+} and a similar trend repeats for most of the cations. Figure 5, right panel, shows a quantitative representation of changes of the relative intensity in the yellow channel of **S4** at magnesium concentrations ranging from 5 μM to 5 mM. The graph inset shows that ca. 50% of the change in the sensor response occurs between 50 and 100 μM. The inset also shows a biphasic behavior in the response probably due to the multiple stoichiometries given by the ditopic nature of the sensor **S4**, which has two 8-HQ sensors (two 8-HQ moieties are attached to the chromophore).

The multidimensional response pattern (18-dimensional, 6 sensors × 3 BGY channels) of the sensor array in the presence of 10 cations (Ca^{2+}, Mg^{2+}, Cd^{2+}, Hg^{2+}, Co^{2+}, Zn^{2+}, Cu^{2+}, Ni^{2+}, Al^{3+}, and Ga^{3+}) was statistically explored using principal component analysis (PCA) and linear discriminant analysis (LDA). PCA is a statistical treatment used to reduce a multidimensional data set for easier interpretation, and is particularly useful for exploratory work. Also, PCA is a nonsupervised method, that is, it does not operate with the information regarding which data points belong to each analyte-cluster, but rather defines the clusters based on their data similarity. Therefore, PCA may be used the test the quality of the data: The fact that the PCA correctly recognizes all of the data points that belong to one analyte (for all analytes tested) would attest to the high discriminatory ability of the array. Here, the data interpretation is based on calculating orthogonal eigenvectors (principal components, PCs) that lie in the direction of the maximum variance within that data set. The first PC contains the highest degree of variance and other PCs follow in the order of decreasing variance. Thus, the PCA concentrates the most significant characteristics (variance) of the data into a reduced dimensionality space. Generally, the higher the number of PCs required to describe a certain level of discrimination, the better the sensor array discriminates between similar analytes.[29] Here, the PCA of the data set (7 trials for each cation) obtained from the 6-sensor array requires 5 dimensions (PCs) out of 17 to describe 95% of the discriminatory range (~30% of all PCs). This level of discrimination is in contrast to those reported for most electronic tongues, which have typically 95% of discrimination in the first two PCs.[30]

(28) Immobilizing of **S2**−**S6** in the polymer matrix at high dilution (0.07% **S2**−**S6** in polyurethane, w/w) also precludes the formation of coordination polymers.

(29) (a) Suslick, K. S. *MRS Bull.* **2004**, *29*, 720–725. (b) Suslick, K. S.; Rakow, N. A. *Tetrahedron* **2004**, *60*, 11133–11138.

(30) (a) Albert, K. J.; Lewis, N. S.; Schauer, C. L.; Sotzing, G. A.; Stitzel, S. E.; Vaid, T. P.; Walt, D. R. *Chem. Rev.* **2000**, *100*, 2595–2626. (b) Gardner, J. W.; Bartlett, P. N. *Electronic Noses: Principles and Applications*; Oxford University Press: New York, 1999.

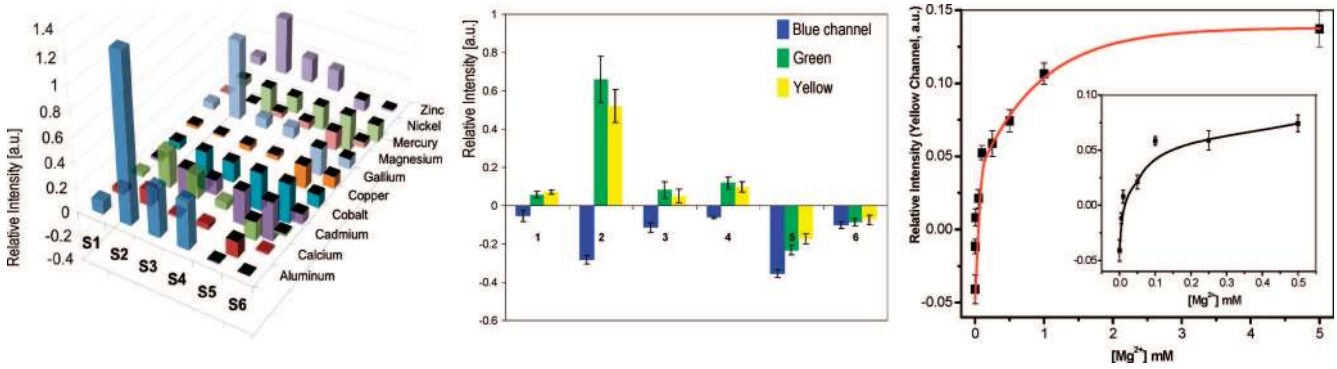

Figure 5. (Left) Response patterns generated by the sensor array (only the green channel) by 10 different metal cations. The black tops in the graph indicate negative responses. (Center) BGY pattern (18-dimensional; 6 sensors × 3 channels) generated by the 6-sensor array upon addition of $MgCl_2$ (1 mM, 200 nL pH 5). (Right) Changes of the relative intensity of **S4** (yellow channel) with increasing Mg^{2+} concentrations. (Inset) Detail of a low concentration (0−500 μM) region.

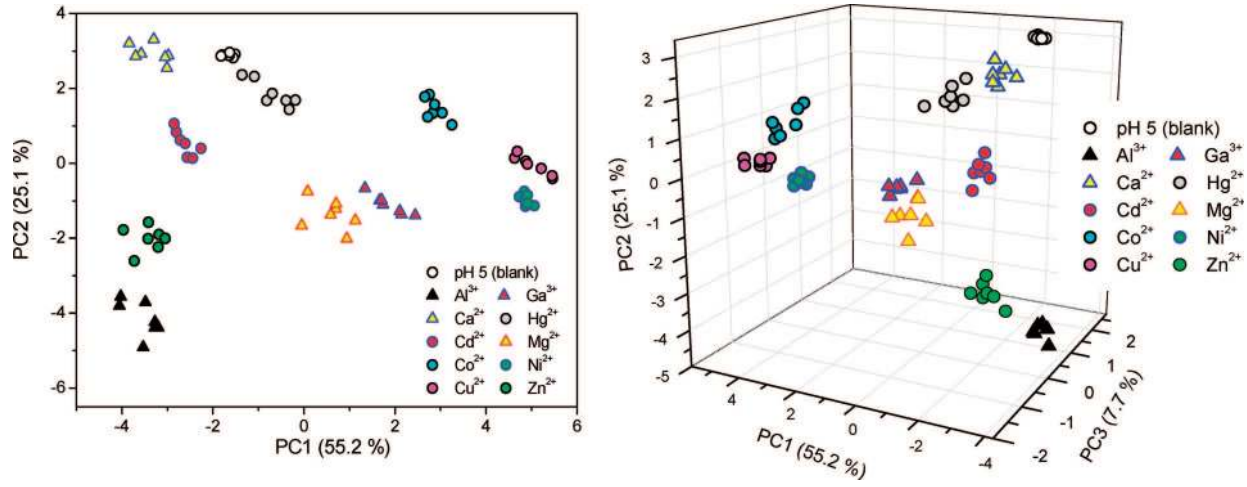

Figure 6. (Left) PCA score plot of the first two PCs describing ca. 80% of the total variance. PCA score plot shows clustering for all 11 samples (7 trials each, 1 mM of their chloride salts, 200 nL, pH 5). (Right) PCA score plot including the third PC describing ca. 8%. The percentage on each axis accounts for the variance intrinsic to the axis.

In addition, each pattern generated by the 6-sensor array is reduced to a single score and plotted in the new space (PC space) generated using the PCs. This representation (score plot) is shown in Figure 6. Here, the PCA score plot utilizes the first two PCs representing 80% of variance and it already shows clear clustering of the data. Furthermore, the high level of dispersion of the data shown by the PCA can be attributed to the high cross-reactivity given by the 8-hydroxyquinoline receptor and the specificity due to the unique photophysical properties generated by the sensor-cation interaction. As we have articulated before, it is the combination of high variability in photonic output and high cross-reactivity in the metal binding by 8-HQ that generates a large difference in the sensor array output and allows for better separation (resolution) of the clusters in the PCA score plot.[16b,c]

Because in most practical applications in chemical sensing one knows which samples belong to the same group (e.g., have the same origin or source), one can use a supervised multivariate method. Linear discriminant analysis (LDA) is a supervised method, i.e. the data points (samples) are defined to belong to certain clusters (analytes) based on their origin, source, time of collection, etc. LDA is similar to PCA in that it also finds linear combinations of features (e.g., sensors responses) which best separate two or more analytes.[21] The main difference is that LDA models the similarities between the data corresponding to the same cluster by introducing the group classification of the trials into the data set. The data are then used as a training set to generate a linear discriminant (LD) function, which describes the best fit parameters to separate different clusters (analytes). The cross-validation (leave-one-out) routine is then used to test the predictability of the sensor array by leaving one observation out of the set at the time, and uses the rest of the data as a training set to generate the linear discriminant function.[31] The LD function is then used to place the excluded observation (data point) within the correct cluster. This is performed for each observation, and the overall ability to classify the observations describes the quality and predictability of the array. Based on the very successful PCA analysis, we were not surprised to learn that the leave-one-out cross validation routine LDA yielded 100% correct classification for all 77 samples.

Part of the motivation of this work was to use the molecular design to generate a significant amount of information with a minimal set of sensor elements in the array, an effort that could provide simple yet effective analytical devices in the near future. Hence, we attempted selecting a subset of sensors that span the 18-dimensional (6 sensors × 3 channels) space generated by all sensors (**S1**-**S6**) while keeping discriminatory capacity. PCA

(31) Supporting Information reports the discriminant functions.

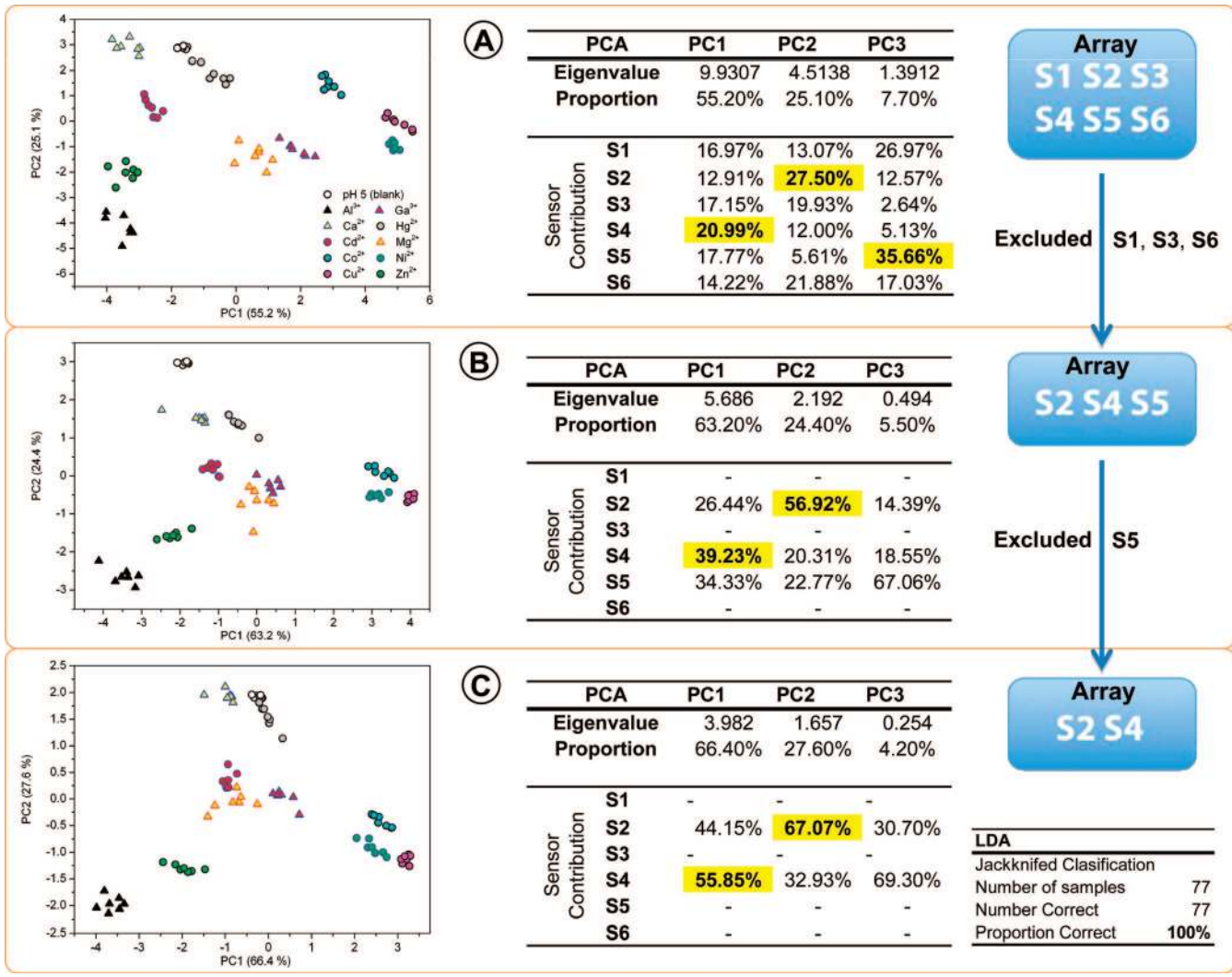

Figure 7. Schematic representation of the rational process for reduction of the number of sensor elements in an array. (A) PCA for the complete set of sensors (**S1**−**S6**) shows that the main contributors for the dispersion are **S4**, **S2**, and **S5** on the PCs with statistical significance. (B) Sensors **S1**, **S3**, and **S5** were excluded from the data set and analyzed again with PCA. PCA shows that the main contributors were **S2** and **S4**. (C) **S3** was excluded from the data and PCA was carried out using the remaining data set. Qualitative inspection of the PCA score plot for the final set of two sensors (**S2** and **S4**) shows clustering of the data without any evident overlap between different samples. Cross-validated LDA shows 100% accurate classification for all three arrays.

has been used in past for a similar purpose.[32,33] The contribution of each individual sensor to the construction of a principal component (axis) can be estimated from the factor loadings. Factor loadings correspond to the cosine of the angle between a principal component axis and the original variable axis. The ideal sensors would be the ones contributing the most to each individual principal component of statistical significance.[32a]

Figure 7 illustrates our approach to reducing the size of the **S1**−**S6** sensor array (Array A). In the experiment aimed at reducing the array, we identified three principal components with statistical significance according to the Kaiser rule. These three PCs represent ca. 90% of the total variance of the six-member array. In these three PCs, **S4** is the main contributor to PC1, **S2** to PC2, and **S5** to PC3 (Figure 7A). Hence, the reduced array was constructed using these three sensors (an optimal subset).

To decrease the size of the array even more, PCA was carried out using the sensors **S2**, **S4**, and **S5** (Array B). Once again, **S2** and **S4** were identified as the most important contributors. This second PCA (Figure 7B) shows **S4** as the main contributor to PC1 and **S2** to PC2. We excluded **S5** and performed the third PCA using the data from just **S2** and **S4**. It is notable that even after excluding the four (**S1**, **S3**, **S5**, **S6**) out of six sensors, the PCA score plot still shows clustering with no evident overlap between the samples (Figure 7C). It is also important that this PCA obtained from the 2-sensor array (Array C: **S2** and **S4**) requires 2 dimensions (PCs) out of 5 to describe 94% of the discriminatory range (~40% of all PCs), demonstrating that the reduction of the number of the sensor elements in the array has not significantly affected the discriminatory performance of the array for this data set containing 11 analytes (10 cations and 1 water pH = 5). Last but not least, LDA using a cross-validation routine was also performed on both reduced arrays (**S2**, **S4**, **S5**

(32) (a) Carey, W.; Beebe, K.; Kowalski, B. *Anal. Chem.* **1986**, *58*, 149–153. (b) Avila, F.; Myers, D.; Palmer, C. *J. Chemometrics* **1991**, *5*, 455–465.

(33) An approach to a size-reduction of a sensor array based on an iterative method rather than a systematic multivariate analysis has also been reported, see: Green, E.; Olah, M. J.; Abramova, T.; Williams, L. R.; Stefanovic, D.; Worgall, T.; Stojanovic, M. N. *J. Am. Chem. Soc.* **2006**, *128*, 15278–15282.

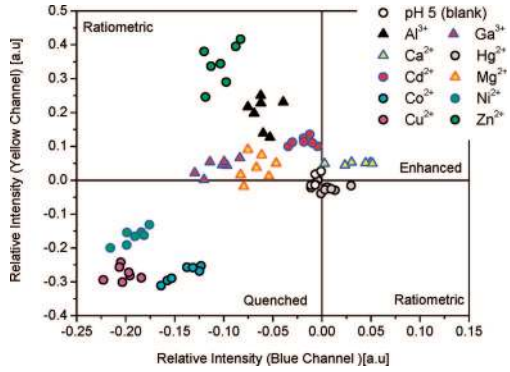

Figure 8. **S4** Raw-data scatter-plot of blue and yellow channels shows clusters of 11 analytes (corresponding to 77 trials, 1 mM of their chloride salts, 200 nL, pH 5).

and **S2**, **S4**) showing 100% correct classification in all 77 cases. It is quite remarkable that just two sensors are capable of differentiating between 11 analytes.

From Figure 7 it can be seen that **S4** is the main contributor to the analyte discrimination in all three arrays A, B, and C. We decided to further explore the source of the "information" provided by **S4**. As mentioned before, each sensor is contributing to the array with three color-emission-channels (**BGY**). Clustering in the three dimensions (**BGY**) can be explored without reduction of the dimensionality by PCA, i.e. we can just plot the raw data. Figure 8 shows a scatter-plot of the two-dimensional raw data corresponding to the relative intensity in the **S4**-blue and **S4**-yellow emission channels. It can be seen that just two channels have already enough information to differentiate between all 11 analytes.

It is important to realize that each of the four quadrants in the scatter plot (Figure 8, left) corresponds to the nature of the signaling in **S4**. For example, the first and third quadrants show analytes that produced enhancement and quenching of the emission in both channels, respectively. Meanwhile, the second and fourth quadrants show the analytes displaying a ratiometric signaling.

The potential practical application of the **S1**−**S6** arrays as well as their minimized versions is tremendous. To illustrate the utility of the above arrays in potential practical application, identification of "enhanced water" drinks based on their Ca^{2+}, Mg^{2+}, and Zn^{2+} cation content was explored. Once again, the process of reducing the number of array members was performed. It was likely that the minimized array would be identical with the previous ones derived for the set of 10 metal cations. This is because the previous array composition was tuned to 10 different cations, including Ni^{2+}, Cd^{2+}, and Hg^{2+}, which are not present in the drinks. The electrolyte and metal ion enhanced waters-beverages used in this test are complex analytes, comprising typically electrolytes (Na^+, K^+, Ca^{2+}, Mg^{2+}), flavoring agents, vitamins, artificial sweeteners, additives such as caffeine, and, last but not least, also Zn^{2+} ions. The list of ingredients for each beverage tested is included in the Supporting Information, including pH values for all beverages.[34] The fingerprint patterns were generated from the enhanced water

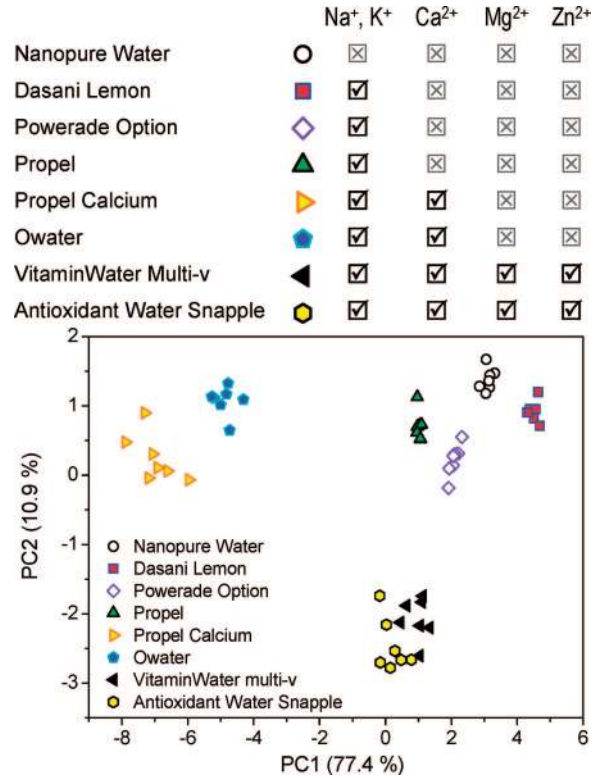

Figure 9. (Top) Samples of enhanced water may be divided into groups by their metal ion content into three groups: A) electrolyte waters free of Mg^{2+}, Zn^{2+} and with no or very low concentration of Ca^{2+}; B) Ca^{2+}-enriched electrolyte waters free of Mg^{2+}, Zn^{2+}; C) electrolyte waters enriched with Ca^{2+}, $Mg^{2+}$and Zn^{2+} (nanopure water is included as a control). (Bottom) PCA score plot of the first two PCs of the **S1**−**S6** array describing ca. 90% of the total variance. PCA score plot shows clustering for all 8 samples (7 trials each); 200 nL of the samples were applied directly from the bottle to each element of the sensor array.

samples without any pretreatment, utilizing chiefly the Ca^{2+}, Mg^{2+}, and Zn^{2+} cation content. Enhanced waters used were: VitaminWater Multi-v (Glaceau Co.), Antioxidant Water Strawberry Acai (Snapple Beverage Corp.), Propel Lemon (Gatorade Co.), Propel Calcium Mixed Berry (Gatorade Co.), Powerade Option Black Cherry (Coca-Cola, Co.), Owater Lemon and Lime (Obeverages, Co.), and flavored water Dasani Lemon (Coca-Cola Co.).[35]

From Figure 9 it is clear that the **S1**−**S6** array sorts the waters based on their cation content. The corresponding PCA score plot shows clear separation of all clusters. Thus, electrolyte waters that do not contain significant amounts of Ca^{2+} and are free of Mg^{2+} and Zn^{2+} (Dasani Lemon, Powerade Option, and Propel Lemon) appear close to the nanopure water. The Ca^{2+} enhanced waters (Propel Calcium and Owater) appear together in the left upper corner, whereas the Ca^{2+}, Mg^{2+}, and Zn^{2+} supplemented waters (Vitaminwater and Antioxidant Water Snapple) appear together in the lower center of the PCA score plot. This pattern is highly consistent with the metal cation content and with the bias of the array sensors elements.

The same reduction of the sensor element number was performed for the enhanced water multianalyte samples, using the same method described in Figure 7. PCA confirmed that sensors **S2**, **S3**, and **S5** provide the highest contributions of

(34) pH values for the enhanced waters range between 3 and 4 for all 7 beverages. Blanks at different pHs (pH 4, 5, and 6) yielded similar responses. This suggests that response patterns generated by samples containing metal ions within this range of pH are mainly due to the presence of metal ions. Also, we did not observe any effect on the solubility of the tested cations within this range of pH.

(35) None of the enhanced waters used contained fluorescent additives or additives capable of significant fluorescence quenching due to energy/electron transfer.

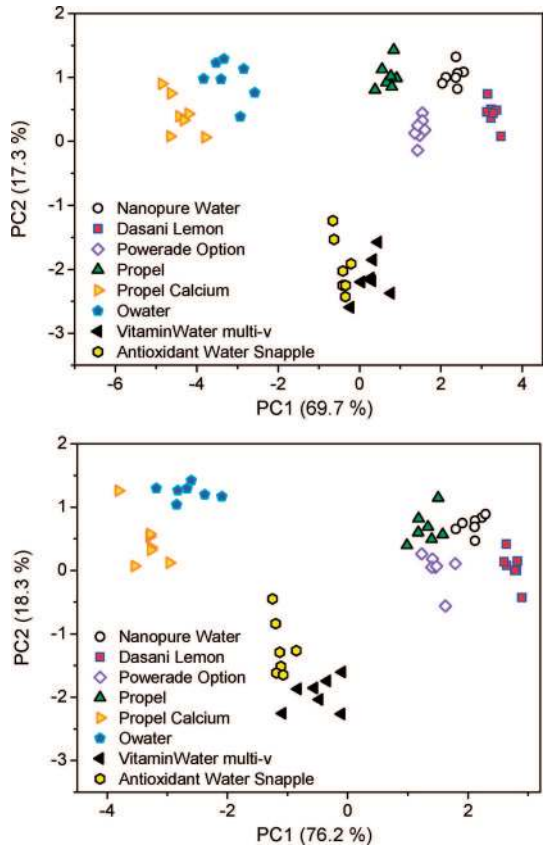

Figure 10. Analyses of the enhanced water samples using arrays with a reduced number of sensor elements. (Top) PCA score plot for the **S2**, **S3**, **S5** array, describing ca. 87% of variance, showing all 56 trials corresponding to the 8 samples. (Bottom) PCA for the **S3**, **S5**, array, describing ca. 95% of variance, showing all 56 trials corresponding to the 8 samples. The cross-validated LDA shows 100% correct classification for all trials.

statistical significance. Also, the **S2**, **S3**, **S5** cross-validated LDA shows 100% accurate classification for all the trials. It is noteworthy that the **S2**, **S4**, **S5** array was also successful and showed 100% accurate classification.

Finally, following the statistical contributions in the PCA, we reduced the array into a two-member **S3**, **S5** array, and performed the PCA and LDA evaluations. Both PCAs corresponding to the **S2**, **S3**, **S5** and **S3**, **S5** arrays are shown in Figure 10. One can see that although both analyses show clear clustering, the discriminative power of the minimized arrays slightly decreases. This is in part due to the multianalyte nature of the enhanced waters as well as the fact that the sensors can respond to only few ions in these complex samples (Ca^{2+}, Mg^{2+} and Zn^{2+}), which limits the principal component space utilized by the analysis. Nevertheless, the **S3**, **S5** cross-validated LDA shows 100% correct classification for all trials. Interestingly, also the previous two-member array (**S2**, **S4**) showed 95% accurate classification. This is because the previous arrays (**S2**, **S4**, **S5** and **S2**, **S4**) were selected for a different set of analytes, that is, the group of 10 metal ions, while the new multicomponent analytes require a slightly modified array. It is important that the described approach to sensor selection and array minimization is general and may be used to match the individual the composition profile of future analytes and multianalytes.

Conclusion

We have demonstrated that the rational design of optical signal transduction in simple luminescent sensors results in a dramatic enhancement of the analytical utility of such sensors and corresponding arrays. This approach utilizes one common receptor, 8-hydroxyquinoline, attached to conjugated fluorophores in such a way that the whole sensor is highly susceptible to change in fluorescence based on the nature of the bound metal. The resulting sensors are highly cross-reactive and provide an information-rich fluorescence output in three (BGY) emission channels, and may be used in both qualitative and quantitative analyses of metal ions. Pattern recognition methods (PCA, LDA) were used to evaluate the analytical utility of the described sensors in arrays. The discriminatory capacity of the arrays was tested on a set of 11 analytes, 10 of which were metal ions. The sensors that contribute most to the analyte discrimination were identified and used to construct yet a smaller and smaller array. A two-member array was found to identify the 11 analytes with 100% accuracy. Finally, the best two of the sensors were tested alone and both were found to be able to discriminate among the samples with 99% and 96% accuracy, respectively. To the best of our knowledge, this is the first time ever reported that one optical sensor element is capable of discriminating among 10 metal ions.

The discriminatory capacity of the described sensors and arrays was also tested on identification of complex analytes such as enhanced water samples comprising various compositions comprising electrolytes, Ca^{2+}, Mg^{2+}, and Zn^{2+} in various levels and proportions. Once again, the present sensors and arrays are capable of discriminating among these complex analytes that were used without any pretreatment. It is noteworthy that the number of sensor elements in the arrays may be reduced using the same method described for metal ion solutions. These results strongly suggest that the sensor selection method is sufficiently general and may be used to generate minimal arrays for various analytes including complex multianalytes such as beverages.[36] The same approach is likely to be useful for the design of sensor arrays for other metal ions. Furthermore, should other receptors be used, it is very likely that the new sensors could also be successfully evaluated using this principle to arrive at performance-optimized arrays utilizing a low number of sensor elements. Finally, it is conceivable that sensors with such a high discriminatory capacity could be used to construct arrays capable of simultaneous qualitative as well as quantitative analyses. This approach to high-performance optical sensors is general, and may be used to generate sensors for other analytes, including anions[16b] and electroneutral molecules.[36,37]

Acknowledgment. P.A. gratefully acknowledges support from the Alfred P. Sloan Foundation, BGSU (Technology Innovations Enhancement grant), and the NSF (CHE #0750303, SENSOR #0330267). M.A.P. acknowledges the support from the McMaster Endowment for a fellowship.

Supporting Information Available: Detailed methodology, response profiles and multivariate analyses (PDF). This material is available free of charge via the Internet at http://pubs.acs.org.

JA802377K

(36) In the specific case of beverages, it would be suitable to include a boronic acid-based sensor for diols to utilize the sugar artificial sweetener (sucralose) content for the analysis. Edwards, N. Y.; Sager, T. W.; McDevitt, J. T.; Anslyn, E. V. *J. Am. Chem. Soc.* **2007**, *129*, 13575–13583.

(37) Zhang, C.; Bailey, D. P.; Suslick, K. S. *J. Agric. Food Chem.* **2006**, *54*, 4925–4931.